

INDUCTIVELY DRIVEN TRANSIENTS IN THE CS INSERT COIL (II): QUENCH TESTS AND ANALYSIS

L. Savoldi @, E. Salpietro # and R. Zanino @

@ Dipartimento di Energetica, Politecnico
Torino, I-10129 Italy

EFDA, Garching, Germany

ABSTRACT

The CS Insert Coil (CSIC), a well-instrumented 140 m long Nb₃Sn solenoid wound one-in-hand and installed in the bore of the CS Model Coil, was tested during the summer of 2000 at JAERI Naka, Japan, within the framework of the International Thermonuclear Experimental Reactor large projects [1]. The maximum transport current in the CSIC was 40 kA and the peak background field was 13 T. The coils were cooled by forced flow HeI nominally at 4.5 K and 0.6 MPa. An inductive heater was used to test stability and quench of the CSIC. In this second of two companion papers we concentrate on the analysis of quench initiation and propagation, based on the study of heater calibration and conductor stability presented in the first paper [2]. The initiation and propagation of an inductively driven quench was tested here for the first time in a two-channel Nb₃Sn conductor, for different transport currents, delay times of the dump, and temperature margins, and a selection of the corresponding results will be presented and discussed. We use the Mithrandir code [3] to analyze this problem and compare the simulation with the experimental results for the evolution of resistive voltage and quench propagation speed, of peak temperature and pressure, and of inlet and outlet mass-flow rate.

INTRODUCTION

Several quench tests were performed on the CSIC with the main purpose of verifying that the conductor conditions (e.g., the maximum temperature) stayed below the threshold specified in ITER design criteria [4]. Of course, being more instrumented (see below) than the CSMC, the CSIC was also an interesting and *first-time* test bed for the study of the thermal-hydraulic behavior of a full-size dual-channel CICC during a quench.

In the past, the Mithrandir code has been validated in detail against quench data [5,6], mainly from QUELL, showing very good accuracy in both resistive voltage and pressure evolution during the transient. However, the QUELL conductor was a sub-size conductor (1/5 of a full-size conductor like the CSIC, without wrappings), and the quenches in QUELL were initiated by using a resistive heater, as opposed (at least in principle, see [2]) to the inductive heater used here. In the CSIC case the Mithrandir analysis may be limited by the assumption of uniform current distribution among the strands, since electromagnetic analysis [7] gives $\sim 1-2$ s from the IH pulse before reaching a uniform current distribution.

Our quench simulations will strongly rely on the inductive heater model and on the calibration of parameters performed within the study of the CSIC stability tests [2]. In these two companion papers, an *integrated* simulation of stability and quench tests in a CICC, i.e., using the same set of input parameters, is performed for the first time to the best of our knowledge.

As a word of caution, it is worth to mention finally that the analysis of the pressure drop in the CSIC [8] shows that the Lorentz forces acting on the conductor at maximum current and field probably caused some displacement/deformation of the cable. Since this effect is not taken into account in our model, except for the use of a friction factor which was developed ad hoc [8], it is not possible here to assess what other influence this could have had on quench initiation and propagation in the CSIC.

EXPERIMENTAL SETUP

The CSIC is shown in FIG 1 together with a sketch of the approximate location of the IH and of the sensors most relevant for the present analysis.

Two types of quench experiments were performed during the CSIC test campaign: 1) those initiated by pulsing an inductive heater (IH) located near the center of the coil (which are summarized in TABLE 1 below), and 2) those initiated by AC losses during

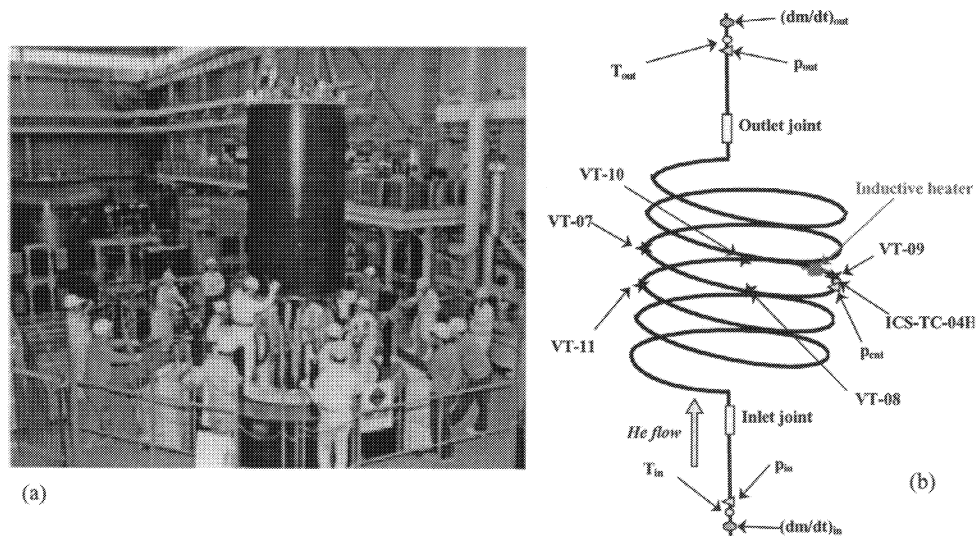


FIGURE 1. (a) CSIC during insertion in the CSMC. (b) Sketch of the CSIC with most relevant sensors and IH location. The actual number of turns is 30.

TABLE 1. Summary of inductively driven quenches in the CSIC (nominal conditions)

Shot No.	Test	I_{CSIC} (kA)	T (K)	dm/dt (g/s)	τ_{D} (s)
174-012	Stability	40	5.3	12	1
176-020	Stability	30	5.3	12	1
178-007	Stability	35	5.3	12	1
181-013	Stability	40	5.3	5	1
185-018	Stability	40	6.8	6	1
210-002	Quench	30	5.3	12	3
216-008	Quench	40	5.3	12	2
218-002	Quench	40	5.3	12	5
221-002	Quench	35	5.3	12	5
223-006	Quench	40	6.8	12	5
343-009	Stability	40	5.3	13	1

ramp-rate limitation tests. All quench experiments in TABLE 1 were performed at nominal $B = 13$ T ($I_{\text{CSMC}} = 44.5$ kA) and $p_{\text{in}} = 0.6$ MPa. The quench detection (threshold) voltage, defining the event as a quench, was set at $QD = 0.1$ V. Once this level was reached, a clock was manually started by an operator (in the quench tests strictly speaking) and after a specified delay time τ_{D} the current in the CSIC was dumped. To limit the peak electro-mechanical load on the CSIC (whose current is inductively increased by the CSMC dump [9]), the dump time constant for the CSIC was significantly shorter than that for the CSMC and the dump circuit was constructed with a small fixed delay between the CSIC dump and the CSMC dump [4]. The simulations presented here will concentrate on the pre-dump phase of a subset of the inductively driven quenches (see TABLE 1). A detailed review of the experimental results of all quenches occurred in the CSIC will be presented elsewhere [4].

MITHRANDIR ANALYSIS AND COMPARISON WITH EXPERIMENTAL DATA

We shall consider here the two quenches of TABLE 1, which are most relevant from a thermal-hydraulic point of view, namely those at highest CSIC current (40 kA) and with longest delay time (5 s): shot 218-002 at high temperature margin (2.5 K nominal) and shot 223-006 at low temperature margin (1 K nominal). Notice (see TABLE 1) that the quenches in shots 174-012, 216-008 and 343-009 are so to say included in the analysis of shot 218-002.

The energy input for the simulations corresponds to the minimum quench energy as computed using the IH model we developed for the stability study [2]: starting from the shape of the current pulse in the heater, the model computes the time and space distribution of the input power in jacket and cable. All parameters used for the present quench simulations are the same as in the stability study; in particular, concerning thermal-hydraulics, friction factors are from [8] and heat transfer coefficients are $\sim 10^3$ W/m²K for bundle-hole heat transfer and $\sim 5 \times 10^3$ W/m²K for helium-solid heat transfer.

As to the boundary conditions to be used in the simulations, it would have been most desirable, within the scope of the present study, to use the experimental pressure values at inlet and outlet, but the traces from ICS-PT-IN and ICS-PT-OUT respectively are very noisy, and even smoothing leaves long wave-length disturbances which appear then as artificial features in the mass-flow rate. We therefore decided to use a simplified model of the external hydraulic circuit, of the kind developed in the past for self-consistent

Mithrandir simulations of quench in QUELL [6]. However, in view of the very limited pressurization in the pre-dump phase of a quench in the CSIC (\sim tenths of a bar, see below), compared to QUELL (\sim bars), it is already clear a-priori that a more sophisticated model of the circuit (e.g., with parallel lines simulating the CSMC conductors) would be needed here, in order to capture the full details of the quench evolution.

Quench at high temperature margin (shot 218-002)

The results of the analysis of the high temperature margin quench are shown in FIG 2.

It may be noticed in FIG 2a that the evolution of the total resistive voltage (from the compensated voltage signal VB-ALL2) starts with a delay of almost 1 s, compared to the 20 ms deposition of energy from the IH. This is due to the fact that most (\sim 95 %) of the input energy goes to the jacket, and it then takes time for heat to diffuse through the jacket thickness and finally to strands/helium [2]. As the voltage reached the 0.1 V level (see above) at $t \sim 3$ s, the clock was started and after $\tau_D \sim 5$ s, i.e., at $t \sim 8$ s, the CSIC current was dumped. In the pre-dump phase the voltage increases almost quadratically with time.

The evolution of the total resistive voltage is well reproduced by the code.

The jacket temperature in FIG 2b is measured with a thermometer mounted to the outer surface of the jacket. This explains the additional ~ 1 s delay between the take-off of the experimentally measured temperature and the initiation of the quench, notwithstanding the proximity of the temperature sensor to the IH.

In the simulation, we had to extend the standard Mithrandir ansatz of uniform temperature in the jacket cross section and include a radial 1D model of heat diffusion in the jacket thickness, as we had done for the IH. With this additional ingredient in the post-processing one sees that a good agreement can be reached in the jacket temperature evolution between simulation and experimental data. The computed *strand* temperature at the sensor location reacts very quickly at the quench onset, while the computed so-called hot-spot (maximum) temperature reacts first to the IH energy input and then, instantaneously, at the quench onset. Unfortunately the differential voltage VD-0910 (obtained from sensors VT-09 and VT-10, see FIG 1b) saturated in this case before the dump, so that it was not possible to reconstruct from a virtual thermometer, see below, an experimental value of the hot-spot temperature.

In FIG 2c the pressurization of helium in the central region of the conductor (i.e., near the IH) shows two different phases: in the first one the pressure rises relatively quickly, then, after the pressure wave induced by the quench has reached the conductor boundaries, also the pressure there begins to increase and helium begins to be expelled more strongly from the outlet (more than twice the nominal mass-flow rate) and also from the inlet (backflow), see FIG 2d. This relief leads to a second phase of the transient with a slower increase of the pressure in the center, and almost constant helium expulsion rate. Notice that the final pressurization before the dump is rather modest (a few tenths of a bar). Indeed, by far the strongest pressurization (~ 2 bar) in the CSIC quenches is reached at the end of the dump phase [4], indicating the dominating role of AC losses over Joule losses.

The qualitative features of the pressure and mass-flow rate evolutions are reproduced by the code, although the code overestimates the rate of increase of the central and boundary pressures. We believe, as discussed above, that these features result mainly from the simplified model of the external hydraulic circuit used for the present simulations. It should also be noticed that the flow-meters are located on pipes several meters upstream

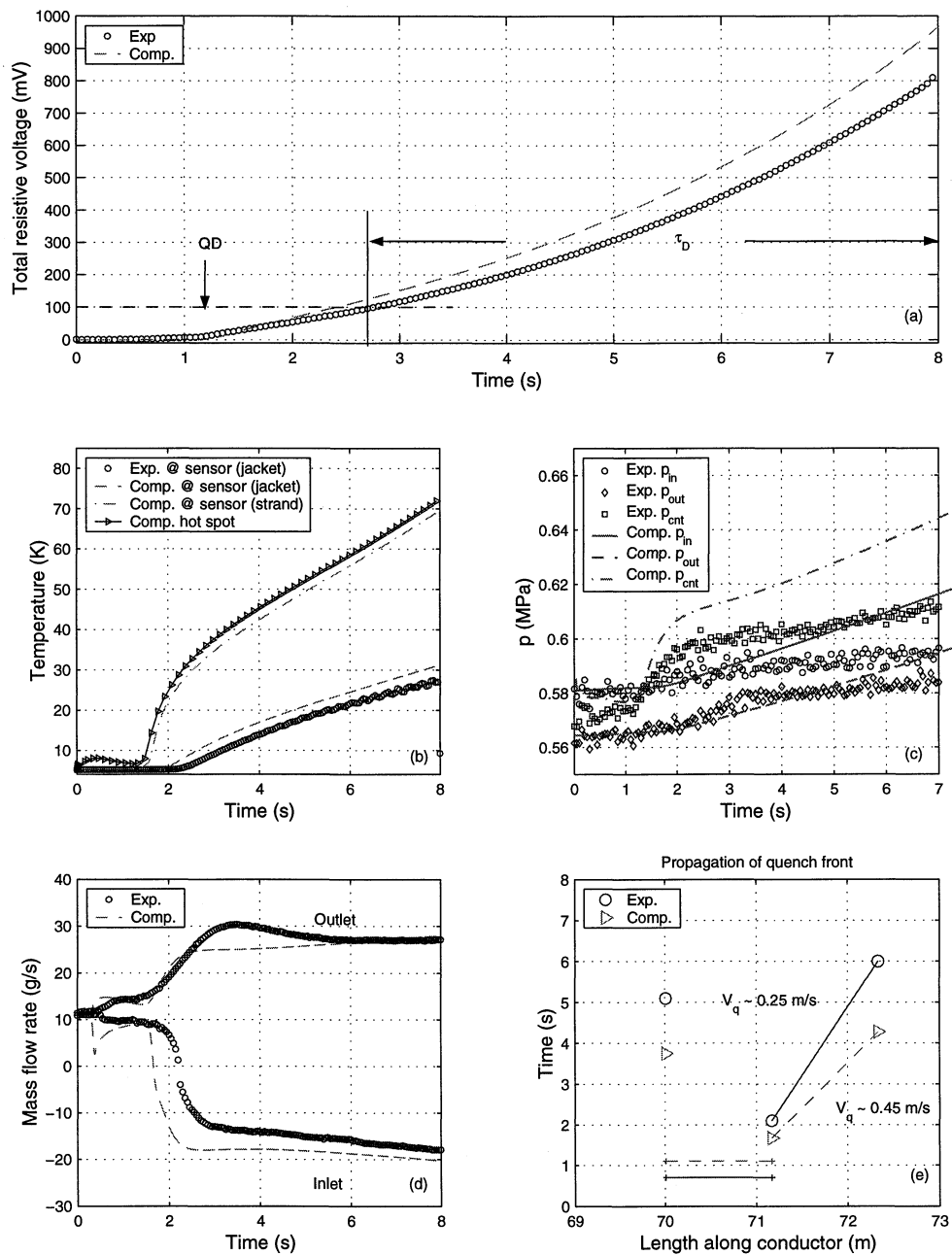


FIGURE 2. Comparison between Mithrandir simulation and experimental data for the pre-dump phase of CSIC quench shot 218-002 ($T = 5.3$ K). Time runs from when the IH was turned on. (a) Evolution of the total resistive voltage; (b) Evolution of the central jacket temperature (sensor ICS-TC-04H about 0.3 m downstream of the IH), of the strand temperature at the same location (computed only), and of the maximum (hot-spot) strand temperature (computed only); (c) Evolution of the central helium pressure (sensor ICS-PT-CNT about 0.3 m downstream of the IH), and of p_{in} and p_{out} (only one data point out of ten is represented from the experimental traces, which had a 5 ms sampling rate); (d) Evolution of inlet and outlet helium mass-flow rates; (e) Evolution of the normal zone reconstructed from voltage take-off at the different voltage taps: the time and approximate location of quench onset are identified by the horizontal segment; the instantaneous location of the quench front at the time it passes by a voltage tap is identified with symbols.

and downstream of the inlet and outlet joints, respectively, which (pipes and joints) are not included in the present simulation. Also, a sudden flow variation appears early in the simulation, when the central pressure spike directly resulting from IH energy input reaches the boundaries, but these spikes are of much smaller amplitude in the experimental data.

In FIG 2e the experimental propagation of the normal zone in the CSIC was determined from the take-off of the signals of the several voltage taps located along the conductor [4]. Before the dump phase, when inductive voltages appear, this is an unambiguous reconstruction of the instantaneous quench front location as it passes through a sensor. It may be noticed that the upstream propagation is slower than the propagation in the downstream direction, as expected.

The agreement between simulation and experiment is fair; the downstream quench propagation speed V_q is overestimated probably due to the above-mentioned overestimate of the central pressurization. Just before dump, the computed V_q turns out to be between the values of the bundle helium speed and of the (bundle+hole) averaged flow speed at the quench front, as peculiar of a pressure-driven quench with finite thermal coupling between bundle and hole.

Quench at low temperature margin (shot 223-006)

For the sake of illustration and comparison we show the results of the analysis of the low temperature margin quench in FIG 3. As the external conditions, e.g., the action of a resistive heater increasing the inlet temperature to the new operating value, are different from the high temperature margin case, different values of the hydraulic circuit parameters, and in particular of the volume of the inlet and outlet manifolds, were used for the simulation of this quench. (Also other authors have simulated this quench with other tools [4], although not in an integrated fashion with the stability problem as done here).

From the comparison of experimental results in FIG 3 and FIG 2 one can see that, except for a faster quench propagation in the low margin case (compare FIG 3e with FIG 2e), which was expected, the qualitative features of the two cases are rather similar. In the low temperature margin case, see FIG 3b, it was also possible to build a “virtual thermometer” from the experimental voltage signals + the temperature dependence of the copper resistance [4], thus reconstructing the evolution of the average temperature between the two voltage taps (VT-09 and VT-10) where also the IH was located. This temperature is defined as the experimental hot-spot temperature and is reported in FIG 3b. A maximum value of 70 K is reached just before dump.

Generally speaking, the agreement between simulation and experiment is somewhat better than in the high temperature margin case. Notice, additionally, the very good agreement with the experimental hot-spot temperature evolution in FIG 3b. As in the high temperature margin case, the computed quench propagation is pressure driven, with V_q from FIG 3e between the values of the bundle helium speed and of the (bundle+hole) averaged flow speed at the quench front.

CONCLUSION AND PERSPECTIVE

Inductively-driven quenches in the CSIC were simulated in an integrated fashion with the stability tests using the Mithrandir code coupled with an electro-magnetic model of the IH. The simulations capture the main features of the experimental results. The quench

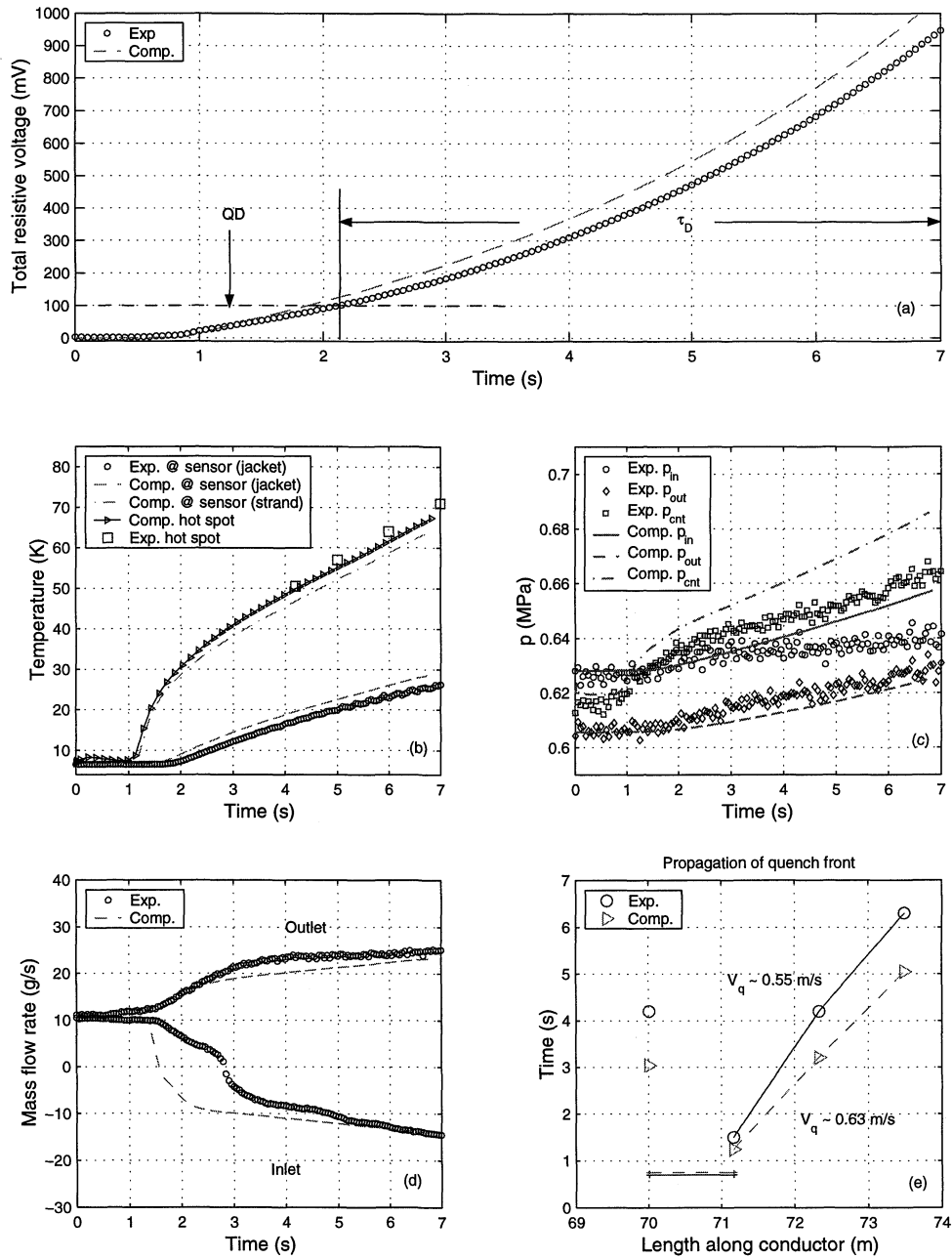


FIGURE 3. Comparison between Mithrandir simulation and experimental data for the pre-dump phase of CSIC quench shot 223-006 ($T = 6.8$ K). Time runs from when the IH was turned on. (a) Evolution of the resistive voltage; (b) Evolution of the central jacket temperature (sensor ICS-TC-04H about 0.3 m downstream of the IH), of the strand temperature at the same location (computed only), and of the maximum (hot-spot) strand temperature; (c) Evolution of the central helium pressure (sensor ICS-PT-CNT about 0.3 m downstream of the IH), and of p_{in} and p_{out} (only one data point out of ten is represented from the experimental traces, which had a 5 ms sampling rate); (d) Evolution of inlet and outlet helium mass-flow rates; (e) Evolution of the normal zone reconstructed from voltage take-off at the different voltage taps: the time and approximate location of quench onset are identified by the horizontal segment; the instantaneous location of the quench front at the time it passes by a voltage tap is identified with symbols.

appears to be pressure driven.

Agreement with experiment in voltage and temperature evolution is good, while the detailed description of the pressure and mass-flow rate transients probably requires a more sophisticated model of the hydraulic circuit. The maximum hot-spot temperature reached in the pre-dump phase of the analyzed quenches with delay $\tau_D = 5$ s was confirmed to be about 70 K.

We plan to implement and validate against CSIC data a model of AC losses in the Mithrandir code [10]. In principle this will allow the study of the current-dump phase of the quench, and of the quenches during ramp-rate limitation tests, which remained beyond the scope of the present paper.

ACKNOWLEDGEMENTS

EFDA and MURST partially financially supported the work of RZ and LS. LS also thanks ASP for support through a post-doctoral fellowship. RZ and LS thank JAERI for the wonderful hospitality provided during the CSIC tests, and P. Michael for reading the manuscript. Discussions with, and data from T. Isono are gratefully acknowledged.

REFERENCES

1. Tsuji, H., Okuno, K., Thome, R., et al., "Progress of the ITER Central Solenoid Model Coil Program", *Nucl. Fusion* **41**, pp. 645-651 (2001).
2. Zanino, R., Carpaneto, E., Portone, A., Salpietro, E., and Savoldi, L., "Inductively driven transients in the CS Insert Coil (II): Heater calibration and conductor stability tests and analysis", presented at the Cryogenic Engineering Conference, July 16-20, 2001, Madison (WI) USA.
3. Zanino, R., DePalo, S., and Bottura, L., "A Two-Fluid Code for the Thermohydraulic Transient Analysis of CICC Superconducting Magnets", *J. Fus. Energy* **14**, pp. 25-40 (1995).
4. Isono, T., Michael, P.C., Takigami, H., and Zanino, R., "Quench of the CS Insert Coil", Section 2.F.ii of the *Cryogenics* Special Issue on CSMC and CSIC Test Results, in preparation.
5. Zanino, R., Bottura, L., and Marinucci, C., "Computer simulation of quench propagation in QUELL", *Adv. Cryo. Eng.* **43**, pp. 181-188 (1998).
6. Savoldi, L., Bottura, L., and Zanino, R., "Simulation of Thermal-Hydraulic Transients in Two-Channel CICC with Self-Consistent Boundary Conditions", *Adv. Cryo. Eng.* **45**, pp. 697-704 (2000).
7. Seo, K., "Estimation of current redistribution after inductive heating by voltage tap signals", presented at the Meeting on CSMC and CSIC Test Results, Naka, Japan, November 9-11, 2000.
8. Zanino, R., Gung, C.Y., Hamada, K., and Savoldi, L., "Pressure drop analysis in the CS Insert Coil", presented at the Cryogenic Engineering Conference, July 16-20, 2001, Madison (WI) USA.
9. Savoldi, L., "Tests and thermal-hydraulic modeling of superconducting magnets for fusion applications", Ph. D. Thesis, Politecnico di Torino, Italy (January 2001).
10. Zanino, R., Savoldi, L., and Zapretalina, E., "Modeling of thermal-hydraulic effects of AC losses in the Central Solenoid Insert Coil using the Mithrandir code", to be presented at the 17-th International Conference on Magnet Technology (MT-17), 24-28 September 2001, Geneva, Switzerland.